

# Chapter 12

## Into the Heart: What Contributions to Cardiac Regeneration?



Alessandra Giuliani and Mara Mencarelli

**Abstract** One of the leading causes of death in the western world is undoubtedly cardiovascular diseases, with special reference to myocardial infarction and consequent heart failure. The therapeutic strategies adopted nowadays are based on drug therapy, coronary artery angioplasty, pacemakers and implantable defibrillator, coronary artery bypass grafts, ventricular remodeling, dynamic cardiomyoplasty, organ transplantation, and mechanical circulatory assistance devices. However, all these procedures are often ineffective and invasive. Moreover, myocardial heart engineering has experienced significant progress over the last 10 years, with fundamental advances in stem cell biology and knowledge of biomaterials. However, one of the limiting factors in the overall interpretation of clinical results obtained by cell therapy is represented by the lack of *in vivo* visualization of the injected cells and of their fate within the myocardium. This chapter shows that X-ray microtomography (microCT) and in particular phase-contrast imaging may offer the unique possibility to detect with high definition and resolution the three-dimensional spatial distribution of stem cells, once injected inside an infarcted heart in small animal models. It was shown, through microCT, the migration of these cells within the damaged cardiac tissue, achieving an appropriate identification and localization of the injected cells. Thus, phase-contrast microCT appears to be an innovative and exclusive way to investigate the cellular events involved in cardiac regeneration and represents a promising tool for future clinical translations.

### 1 Introduction

One of the leading causes of death in the western world is undoubtedly cardiovascular diseases (CVDs), with special reference to myocardial infarction (MI) and consequent heart failure (HF) [1–3], caused by irreparable loss or dysfunction of

---

A. Giuliani (✉) · M. Mencarelli  
Department of Clinical Sciences, Polytechnic University of Marche, Ancona, Italy  
e-mail: [a.giuliani@univpm.it](mailto:a.giuliani@univpm.it)

cardiomyocytes due to the abrupt deprivation of oxygen supply. In this context, with only small fractions of myocytes retaining the capacity to replicate, the heart has a very limited self-regeneration capacity.

Thus, the therapeutic strategies adopted nowadays for HF are based on drug therapy, coronary artery angioplasty (using balloons and stents), pacemakers and implantable defibrillator, coronary artery bypass grafts, ventricular remodeling, dynamic cardiomyoplasty, organ transplantation, and mechanical circulatory assistance devices. However, all these procedures are often ineffective and invasive.

On the other hand, considerable progress has been made in myocardial heart engineering over the last 10 years, with fundamental advances in stem cell biology and knowledge of biomaterials.

Unfortunately, despite these advantages, clinical trials applying myocardial heart engineering have shown contradictory results, with moderate or no evident benefits for patients.

These approaches were mainly based on cellular therapy with the objective to generate new myocardium by transcatheter and intramyocardial cell injection, mainly of bone marrow [4] and skeletal muscle [5] origin. However, despite the limited positive impact on cardiac repair [6], these studies demonstrated a positive impact on patients with chronic MI and HF, with negligible adverse effects and without significant increase of arrhythmias [7].

Resident cardiac progenitor cells (CPCs) are an alternative cell source with which to treat ischemic cardiomyopathies. Indeed, progenitor cells living in the heart are programmed to generate the myocardium, i.e., the tissue lost with MI [8–13]. Cardiac mesenchymal stem cells (MSCs) [14] are a special type of resident cells, recently found in the cardiac stroma [15], referred to in the literature as cardiac mesenchymal stemlike cells [16] or cardiac mesenchymal-like stromal cells [17, 18].

However, detection of these injected cells within the myocardium is still a challenge, independently of their origin, because a reliable reconstruction of their fate is hampered by the lack of an efficient method for their 3D imaging and quantification within the heart.

Light, fluorescence, scanning, and transmission electron microscopy techniques efficiently image and quantify the tissue-rebuilding process but have the limitation of delivering only 2D local information, thus hampering their applicability for cell tracking, as shown by Terrovitis et al. [19]. Indeed, as only a few sections per sample are typically analyzed, the quantitative evaluation is often subjected to variability and sampling errors.

Moreover, 3D imaging methods, like MRI, PET, and conventional CT, despite having been shown to provide reliable quantification of the rebuilding process (including longitudinal cell tracking), introduce different limitations in the localization of the injected cells within the heart, mainly due to the need to use contrast agents [19, 20].

## 2 Synchrotron Radiation-Based Imaging of Stem Cell Homing in Infarcted Hearts

Third-generation synchrotron structures, producing brilliant photon beams, with spatial and temporal coherence properties [21, 22], have proved extremely useful for studying *ex vivo* the myocardium in animal models [23–25] and humans [26].

These studies demonstrated that image quality and quantitative information are sensibly improved by the use of phase-contrast microtomography (PhC-microCT). As fully described in the previous chapters, while in conventional microCT the signal is exclusively based on attenuation contrast, in the PhC approach both the amplitude and the phase of the X-ray wave are modified when passing through a tissue. This effect is described by the refractive index  $n$ :

$$n(\mathbf{r}) = 1 - \delta(\mathbf{r}) + i\beta(\mathbf{r}) \quad (12.1)$$

The  $\delta$  value, the refractive index decrement, is actually proportional to the mean electron density, which in turn is almost proportional to the mass density. It is much larger than  $\beta$ , the attenuation index, at the energies used to study soft tissues, with the  $\delta/\beta$  ratio close to  $10^3$ .

The novelty that differentiates the phase-contrast method from the conventional absorption-based one is the capacity of the first in discriminating tissues with similar attenuation [27], like myocardial structure, coronary vessels, and conduction bundle.

Kaneko et al. [26] imaged all these structures on five non-pretreated whole infantile and fetal heart specimens obtained by autopsy. The study was carried out at the SPring-8 synchrotron radiation facility using the Talbot grating interferometer at the bending magnet beamline BL20B2 and demonstrated that PhC-microCT could be a powerful tool for elucidating unanswered questions concerning congenital heart diseases.

Dullin et al. [23] depicted the same conclusion on animal models: they attempted a phosphotungstic acid (PTA) *ex vivo* staining approach with the objective to efficiently enhance the X-ray attenuation of soft tissues for a better visualization of mouse hearts by microCT. This study demonstrated that the technique allowed the *ex vivo* imaging of several structures (atrium, ventricles, fiber structure of the myocardium, vessel walls) of PTA-stained mouse hearts, not requiring monochromatic and/or coherent X-ray sources. Moreover, by volumetric measurements, they were able to assess the plaque volumes in the aortic valve region of mice from ApoE<sup>-/-</sup> mouse models.

Some authors [24] recently showed that microCT offers the possibility of visualizing in 3D and in *ex vivo* conditions, with high definition and resolution, rat cardiac progenitor cells (CPCs) after injection in infarcted rat hearts. Myocardial infarction was induced by coronary binding of the left anterior descending coronary artery in the male Wistar rats (*Rattus norvegicus*). Three weeks later,  $5 \times 10^5$  rat clonogenic

CPCs, previously labeled with iron oxide (Feridex) nanoparticles, were injected intramyocardially in the rat hearts. Sham-operated rats were treated similarly, but without tying a ligature around the artery. One week later, the animals were sacrificed and the hearts were fixed for the microCT analysis.

The microCT acquisitions were performed at the beamline BM05 of the European Synchrotron Radiation Facility (ESRF), using a 15 keV monochromatic X-ray beam, at two different sample-to-detector distances: 25 mm and 500 mm to achieve both the absorption- and the phase-contrast signal.

A full fusion automatic algorithm described elsewhere [28] was used to superimpose the two sets of data, merging them in a single image dataset for further 3D visualization.

The injected cells were observed in 3D, after migration to the damaged cardiac tissue, with structural information not previously imaged by conventional 2D imaging techniques.

The X-ray absorption of cells labeled with iron oxide was higher than for the surrounding hosting tissues, allowing their discrimination as bright spots in the reconstructed volumes (Fig. 12.1). One week after the injection, the labeled cells were mostly found in the infarcted area (Fig. 12.1c, d, f), indicating their migration from the injection site, close to the coronary binding, toward the damaged tissue. The fingerlike cell structures detected in the left ventricular wall (Fig. 12.1d, f) constitute another morphological finding that was never observed by histological methods. Moreover, single smaller units were also found in the atria, in large vessels (Fig. 12.1c, e), and in the right ventricle (Fig. 12.1c).

This study first showed that microCT offers the possibility of obtaining 3D visualization of the cell spatial distribution and a quantification of the number of cells that are able to migrate from the site of injection to different areas of the rat heart tissue, with special reference to the infarcted myocardium. Notably, this microCT approach was validated by two independent methodologies of cell tracking based on quantum dots labeling and genetically engineered EGFP cells.

However, imaging by microCT of soft structures, like those present in an engineered heart, remains challenging, and often phase-contrast settings are preferred to conventional attenuation contrast because of their superior sensitivity. Thus, being unclear which phase tomography method could produce more significant results, some authors [29] recently imaged a rat heart, comparing the performances of three phase tomography methods implemented at the beamline ID19 of the ESRF. They tested the X-ray grating interferometry (XGI) and two propagation-based settings, i.e., the one based on a single sample-detector distance (SD-PhC) and the holography (HT), described in detail in the previous chapters. They found that, even if the XGI data generally exhibit much better contrast-to-noise ratios, the spatial resolution available to detect the morphological features was about a factor of two better for HT and SD-PhC compared to XGI.

In this direction, Izadifar [30] recently explored synchrotron radiation phase-contrast methods to image and quantify the efficiency of 3D-printed cardiac patches implanted in a rat myocardial infarction model. Indeed, another objective of cardiac tissue engineering is the development of implantable constructs and of cardiac patches, which provide physical and biochemical cues for myocardium regeneration.

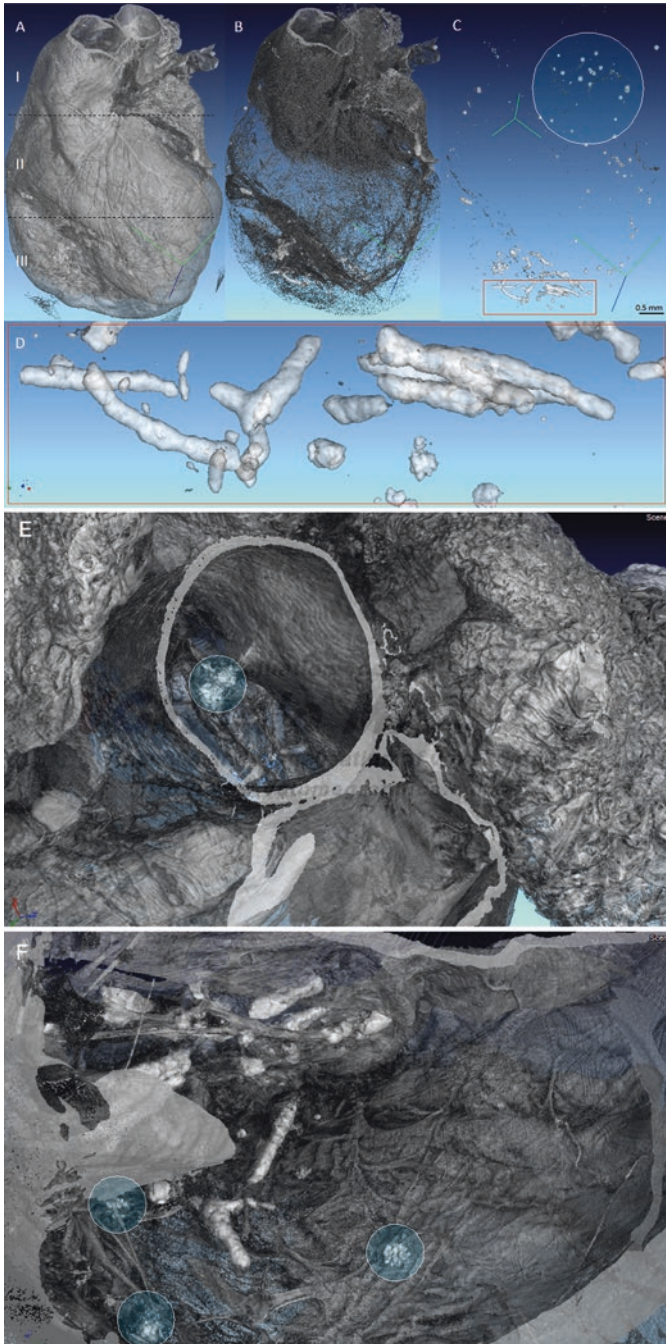


**Fig. 12.1** MicroCT reconstruction of an infarcted rat heart injected with  $5 \times 10^5$  rat CPCs [24]. (a) 3D image as produced using the full fusion algorithm. By segmentation, it is possible to achieve information on the internal structure of the heart (b) and the distribution of labeled cells (c, d). 3D reconstructions of two different regions of interest: (e) atria and large vessels; (f) infarcted ventricle. Lighted circles facilitate the recognition of the CPCs

In this study [30], innovative nanoparticles expected to modulate the temporal control of growth-factor (GF) release in cardiac patches were successfully developed. Propagation-based PhC-microCT was performed at BMIT-BM beamline of the Canadian Light Source (CLS), using a 25 keV beam energy and three distinct phase propagation distances of 22 cm, 76 cm, and 147 cm. Images obtained by phase retrieval showed and quantified the microstructural features of fibrin and alginate, which were low-density (>97% water) constituents of the patch. Moreover, several anatomical details, including the microvessels surrounding the implanted patch, were observed.

Remarkably, the morphometric information on patch and heart was achieved without using any contrast agent, suggesting that the PhC-microCT could play a key role in quantitative monitoring, in a nondestructive way, of these engineered bio-constructs.

### 3 Phase-Contrast Imaging to Evaluate Stem Cell Therapy: An Intriguing Hypothesis

The available imaging methodologies, including microCT, still present problems to be solved before translating myocardial regeneration on clinical grounds [19, 20]. In stem cell therapy, when cells injected in the ischemic tissue are preventively labeled with contrast agents, these techniques often proved to be unable to quantify cell engraftment, because of the injected cells' proliferation and the consequent underestimation caused by the hyper-dilution below the detection limit or by unequal distribution of the tracer on dividing cells. Moreover, Gianella et al. [31] evidenced the activation of macrophages when injecting endothelial progenitors, previously loaded with iron oxide nanoparticles, into ischemic tissues. Indeed, dying cells release these tracers, afterward taken up by macrophages.

A few years ago, Albertini et al. [32] used the PhC-microCT for the first time to visualize in 3D the extracellular matrix (ECM) organization after *in vitro* seeding of bone marrow-derived human and murine mesenchymal stem cells, induced to myogenic differentiation and labeled with iron oxide nanoparticles, onto polyglycolic acid-poly(lactic acid) scaffolds (PGA-PLLA).

Another study performed by Zehbe et al. [33] first observed microCT efficiency in tracking unlabeled stem cells when seeded onto a scaffold. Their study, performed by synchrotron radiation-based microCT, had the purpose of testing a method for the control of neuronal cell growth through the application of an electrical potential. The authors expected to observe only strongly absorbing deposited gold structures and weakly absorbing polymer substrates, but, unexpectedly, also the unlabeled cells were well imaged and with a distribution in agreement with the fluorescence microscopic images acquired previously.

More recently, Giuliani et al. [34] adopted the same PhC-microCT protocol used in [32] to study *in vitro* cultures of endothelial colony-forming cells (ECFCs) from healthy controls and patients with Kaposi sarcoma and human CD133+

muscle-derived stem cells seeded onto PGA-PLLA. In this case, the structural organization of cells on the bioscaffold was imaged and the rate at which cells modified the construct at different time points from seeding was quantified.

The three previously reported studies inspired a fourth study [20], a demonstrative investigation in which the appropriateness of the X-ray PhC-microCT approach to track unlabeled cells within the myocardium was discussed.

When studying, by microCT, tissues predominantly made of atoms with low atomic number  $Z$  (like the myocardium), phase-contrast approaches are often preferred to conventional absorption-based ones because of their greater sensitivity, as discussed in detail in some of the previous chapters. Moreover, mismatches in shape and integration between the regular pattern of a tissue and embedded different structures also lead to PhC-microCT reconstructions with highly improved contrast between these different phases: this is the case of stem cells injected in an infarcted heart that migrate in the damaged myocardium.

Figure 12.2 shows how it is possible to visualize and track unlabeled cells within the myocardium by X-ray PhC-microCT. The cardiac progenitor cells (CPCs), at early stages after the injection, are still undifferentiated and not integrated with the hosting tissue, as shown in Fig. 12.2a-I. In propagation-based PhC-microCT, the detector is placed at a suitable distance from the sample in order to allow the detection of the typical edge-enhanced profile of the CPCs (Fig. 12.2a-II). Thus, as shown in the 3D reconstruction of a rat heart subvolume of Fig. 12.2a-III (inner wall of the infarcted left ventricle), the unlabeled CPCs are clearly visible inside the damaged ventricle, as indicated by the red arrows [20]. Several tests showed that this finding, unexpected and new, was attributable to phase-contrast phenomenon. Indeed, propagation-based PhC-microCT enabled to track the CPCs at different time points, allowing to obtain the same information on the kinetics, previously exclusively supported in the literature by 2D microscopy analysis [20].

Briefly, ten Wistar male rats were submitted to a ligature around the left descending coronary vessel in order to induce a myocardial infarction in the left ventricle. After 3 weeks,  $5 \times 10^5$  stem cells were directly injected in the ligature site: five rats were injected with rat cardiac progenitor cells (rCPCs), the remaining five with the analogue quantity of human cardiac stromal cells (hCStCs). The rCPCs and the hCStCs were obtained from atrial auricle of Wistar rats and donor patients undergoing cardiac surgery (i.e., aortic valve replacement, coronary artery bypass), respectively [17, 20]; in some animals, cells labeled with iron oxide nanoparticles (Feridex) were injected; in others, prior to injection, the cells were cultured with the growth factor of insulin-transferrin-sodium selenite (ITS) or in total absence or with combined use of Feridex and ITS. Times to sacrifice after injection were the following ones: 24–48 h, 12–13 days, 21 days, and 30 days. The microCT experiments were carried out at the ID19 beamline of the ESRF using a 15 keV X-ray energy and a distance between sample and detector of 25 mm.

The sections obtained at 25 mm for an infarcted rat heart injected with unlabeled CPCs showed the presence of very contrasted structures (white spots), mainly concentrated in the infarcted area (Fig. 12.2b). This contrast is not justified by physical phenomena due to X-ray absorption since the injected cells had not been marked

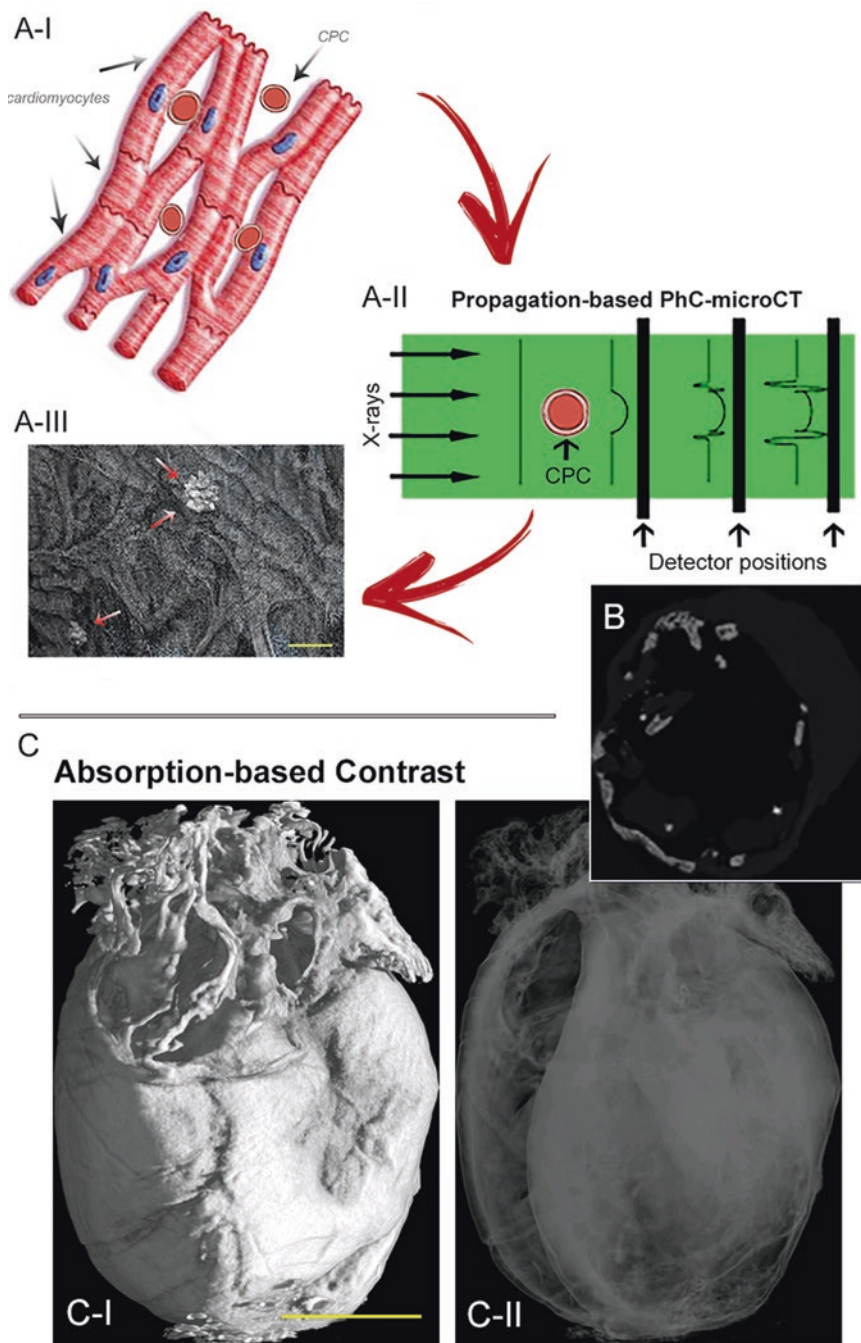


**Fig. 12.2** Phase-contrast ability of visualizing the injected cardiac progenitor cells (CPCs) into the rat myocardium [20]. (a-I) The cells, early after their injection, are still undifferentiated and not integrated in the hosting myocardium; (a-II) edge-enhanced profile of the CPCs when the



with any contrast agent and the sample preparation procedure was not affected by the presence of contaminants with high atomic number  $Z$ . Indeed, a not-infarcted rat heart, injected with only vehicle saline solution (but without cells) and sacrificed using an identical protocol, did not present any contrast signal [25]. Another study involving differential imaging [35] of sequential axial slices further confirmed that the observed signal is due to phase contrast (data not shown). Moreover, conventional microCT, based on the mapping of the absorption contrast, furtherly confirmed that the white spots were due to phase contrast. Indeed, an infarcted rat heart injected with  $5 \times 10^5$  unlabeled rCPCs was studied by means of a SkyScan 1174 (Bruker, Kontich, Belgium): as shown in Fig. 12.2, panel c–II, the strong contrast is no longer present in the 3D reconstruction, when the myocardium has been virtually rendered translucent to visualize the internal structures.

Some microCT images of rat hearts injected with unlabeled CPCs are shown in Fig. 12.3a–c: the signal depicted in magenta was attributed to the injected cells for many reasons. Firstly, the analysis of a noninfarcted rat heart injected with the same amount of CPCs revealed an analogue signal, even if more homogeneous and diluted (data not shown). Moreover, the quantitative results obtained in the study on the ten rats (Fig. 12.3d) further confirmed this evidence [20].

Based on these observations and the deriving quantitative analysis, Giuliani et al. [20] formulated the following hypothesis:

1. PhC-microCT is capable of discriminating the injected cells from the myocardium: the reason can lie in the electron density difference between undifferentiated (injected) and differentiated cells (the myocardium) and/or to mismatches in integration between the regular pattern of the myocardium and the injected cells before their engraftment.
2. The aggregate cell volume increases up to 21 days from cell injection, possibly due to injected cell proliferation and/or the activation of the endogenous stem cells.
3. The aggregate cell volume decreases from 21 to 30 days after cell injection, possibly indicating the beginning of differentiation/cell engraftment of the injected cells. This hypothesis is supported by Rossini et al. [17] who found in the same rat model of chronic MI, after 21 days from hCStC injection, a portion of them showing sarcomere striation and volume compatible with that of adult cardiomyocytes.
4. Feridex labeling was confirmed to interfere with the regeneration process activated by the CPCs, possibly because of macrophage action previously described [31].
5. ITS seems to favor tissue regeneration by supporting cell engraftment [19] and CPC proliferation.

←  
**Fig. 12.2** (continued) detector is placed at a suitable distance from the sample in a propagation-based PhC-microCT setting; (a–III) 3D reconstruction of the inner wall of the infarcted left ventricle of a rat: the injected (unlabeled) CPCs are clearly visible and indicated by the red arrows. Bar, 50  $\mu\text{m}$ . (b) An axial slice of the infarcted rat heart treated with unlabeled rCPCs. It was reconstructed without the application of the Paganin filter to evaluate the edge enhancement. (c) Infarcted rat heart injected with unlabeled rCPCs: conventional (absorption-based) microCT analysis. Solid (c–I) and semitransparent (c–II) 3D reconstructions. The unlabeled CPCs are not visible anymore. Yellow bar, 300  $\mu\text{m}$

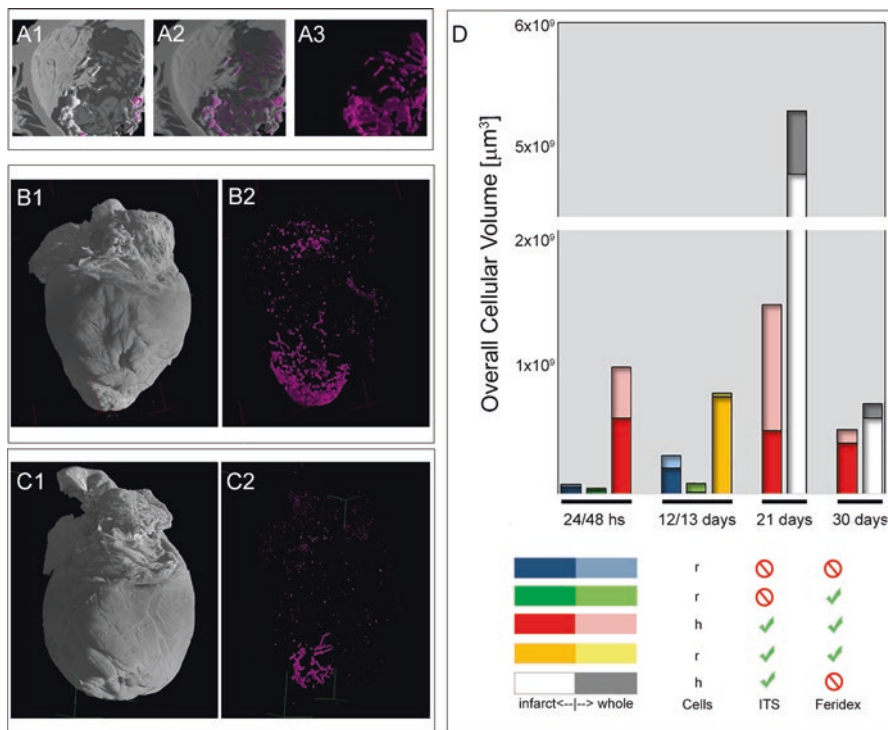


**Fig. 12.3** MicroCT 3D reconstructions of the infarct in a rat heart injected with unlabeled hCStCs (**a1–a3**) and of the entire hearts when injected with hCStCs, previously cultured with ITS and without Feridex (**b1–b2** at 21 days, **c1–c2** at 30 days from cell injection) [20]. Gray myocardium, magenta hCStCs. (**d**) Quantitative results. *h* human-derived CStCs, *r* rat-derived CPCs

## 4 From Stem Cell Therapy to Heart Engineering: The New Frontiers

Myocardium engineering by cell therapy still requires further research, mainly focused on the objective to improve cell delivery methods, before its introduction for drug screening and patient-specific disease modeling [36]. Indeed, it was found that transplanted cells are not able to survive for long periods because of pathologically modified extracellular matrix (ECM), proapoptotic factors, and inflammatory response. Thus, testing of antioxidant, anti-inflammatory, angiogenic, and antiapoptotic products should be performed in order to favor the survival of transplanted cells.

In this direction, porous biomaterials should offer a suitable microenvironment for cell survival and function, mimicking the natural extracellular environment. Natural and innovative synthetic biomimetic scaffolds are under investigation with the main objective to allow cell attachment and their colonization and, by their

grafting to the damaged myocardium, to achieve a modulated delivery of such cells, releasing biochemical factors and nutrients. For instance, a polyglycerol sebacate (PGS) matrix was recently developed for cardiac patch application with the objective of supporting the adhesion and growth of rat and human cardiac progenitor cells [37].

Synchrotron radiation-based PhC-microCT techniques are expected to give an invaluable support in this direction, elucidating unanswered questions concerning the kinetics of tissue repairing.

However, preclinical application of PhC-microCT for the *vivo* imaging of small animal hearts is nonetheless challenging because scan times are still longer than a single respiratory or cardiac cycle. To overcome this problem on rodent models, Holbrook et al. [38] recently proposed two strategies for cardiac gating in dual-source, preclinical microCT: fast prospective gating (PG) and uncorrelated retrospective gating (RG). These methods combined with a sophisticated iterative image reconstruction algorithm provided faster acquisitions and high image quality in low-dose 4D (i.e., 3D + Time) cardiac microCT.

Clinical application of PhC-microCT is also gaining traction [39], even if the *in vivo* imaging of the heart remains challenging also in this case. Indeed, as the heart is surrounded by the air-filled alveoli of the lungs, artifacts caused by X-ray refraction could emerge [26], and the strong X-ray absorption of the ribs could reduce the detection of phase-shift values inside compared to an isolated heart.

Thus, future development of the PhC-microCT systems and methods for *in vivo* human heart imaging are expected in the coming few years.

## References

1. Roger VL (2013) Epidemiology of heart failure. *Circ Res* 113:646–659
2. Mozaffarian D, Benjamin EJ, Go AS, Arnett DK, Blaha MJ, Cushman M, de Ferranti S, Després JP, Fullerton HJ, Howard VJ, Huffman MD, Judd SE, Kissela BM, Lackland DT, Lichtman JH, Lisabeth LD, Liu S, Mackey RH, Matchar DB, McGuire DK, Mohler ER 3rd, Moy CS, Muntner P, Mussolino ME, Nasir K, Neumar RW, Nichol G, Palaniappan L, Pandey DK, Reeves MJ, Rodriguez CJ, Sorlie PD, Stein J, Towfighi A, Turan TN, Virani SS, Willey JZ, Woo D, Yeh RW, Turner MB (2015) Heart disease and stroke statistics – 2015 update: a report from the American Heart Association. *Circulation* 131(4):e29–e322 Corrigendum: (2015). *Circulation*, 131, e98; *Circulation*, 131, e117; *Circulation*, 131, e163; *Circulation*, 131, e319
3. Benjamin EJ, Blaha MJ, Chiuve SE, Cushman M, Das SR, Deo R, de Ferranti SD, Floyd J, Fornage M, Gillespie C, Isasi CR, Jiménez MC, Jordan LC, Judd SE, Lackland D, Lichtman JH, Lisabeth L, Liu S, Longenecker CT, Mackey RH, Matsushita K, Mozaffarian D, Mussolino ME, Nasir K, Neumar RW, Palaniappan L, Pandey DK, Thiagarajan RR, Reeves MJ, Ritchey M, Rodriguez CJ, Roth GA, Rosamond WD, Sasson C, Towfighi A, Tsao CW, Turner MB, Virani SS, Voeks JH, Willey JZ, Wilkins JT, Wu JH, Alger HM, Wong SS, Muntner P, American Heart Association Statistics Committee, Stroke Statistics Subcommittee (2017) Heart disease and stroke statistics-2017 update: a report from the American Heart Association. *Circulation* 135(10):e146–e603. <https://doi.org/10.1161/CIR.0000000000000485>

4. Strauer BE, Steinhoff G (2011) 10 years of intracoronary and intramyocardial bone marrow stem cell therapy of the heart: from the methodological origin to clinical practice. *J Am Coll Cardiol* 58:1095–1104
5. Menasché P, Alfieri O, Janssens S, McKenna W, Reichenspurner H, Trinquart L, Vilquin JT, Marolleau JP, Seymour B, Larghero J, Lake S, Chatellier G, Solomon S, Desnos M, Haggège AA (2008) The myoblast autologous grafting in ischemic cardiomyopathy (MAGIC) trial: first randomized placebo-controlled study of myoblast transplantation. *Circulation* 117:1189–1200
6. Sanganalath SK, Bolli R (2013) Cell therapy for heart failure: a comprehensive overview of experimental and clinical studies, current challenges, and future directions. *Circ Res* 113:810–834
7. Fisher SA, Doree C, Mathur A, Martin-Rendon E (2015) Meta-analysis of cell therapy trials for patients with heart failure. *Circ Res* 116:1361–1377
8. Chamuleau SA, Vrijisen KR, Rokosh DG, Tang XL, Piek JJ, Bolli R (2009) Cell therapy for ischaemic heart disease: focus on the role of resident cardiac stem cells. *Neth Heart J* 17:199–207
9. Frati C, Savi M, Graiani G, Lagrasta C, Cavalli S, Prezioso L, Rossetti P, Mangiaracina C, Ferraro F, Madeddu D, Musso E, Stilli D, Rossini A, Falco A, Angelis AD, Rossi F, Urbanek K, Leri A, Kajstura J, Anversa P, Quaini E, Quaini F (2011) Resident cardiac stem cells. *Curr Pharm Des* 17:2074–2099
10. Leri A, Kajstura J, Anversa P (2011) Role of cardiac stem cells in cardiac pathophysiology: a paradigm shift in human myocardial biology. *Circ Res* 109:941–961
11. Li TS, Cheng K, Malliaras K, Smith RR, Zhang Y, Sun B, Matsushita N, Blusztajn A, Terrovitis J, Kusuoka H, Marbán L, Marbán E (2012) Direct comparison of different stem cell types and subpopulations reveals superior paracrine potency and myocardial repair efficacy with cardiosphere-derived cells. *J Am Coll Cardiol* 59:942–953
12. Nadal-Ginard B, Ellison GM, Torella D (2014) The cardiac stem cell compartment is indispensable for myocardial cell homeostasis, repair and regeneration in the adult. *Stem Cell Res* 13:615–630
13. Savi M, Bocchi L, Rossi S, Frati C, Graiani G, Lagrasta C, Miragoli M, Di Pasquale E, Stirparo GG, Mastroianni G, Urbanek K, De Angelis A, Macchi E, Stilli D, Quaini F, Musso E (2016) Antiarrhythmic effect of growth factor-supplemented cardiac progenitor cells in chronic infarcted heart. *Am J Physiol Heart Circ Physiol* 310(11):H1622–H1648. <https://doi.org/10.1152/ajpheart.00035.2015>
14. Leite CF, Almeida TR, Lopes CS, Dias da Silva VJ (2015) Multipotent stem cells of the heart—do they have therapeutic promise? *Front Physiol* 6:123. <https://doi.org/10.3389/fphys.2015.00123>
15. Chong JJ, Chandrakanthan V, Xaymardan M, Asli NS, Li J, Ahmed I, Heffernan C, Menon MK, Scarlett CJ, Rashidianfar A, Biben C, Zoellner H, Colvin EK, Pimanda JE, Biankin AV, Zhou B, Pu WT, Prall OW, Harvey RP (2011) Adult cardiac-resident MSC-like stem cells with a proepicardial origin. *Cell Stem Cell* 9:527–540. <https://doi.org/10.1016/j.stem.2011.10.002>
16. Ryzhov S, Sung BH, Zhang Q, Weaver A, Gumina RJ, Biaggioni I, Feoktistov I (2014) Role of adenosine A2B receptor signaling in contribution of cardiac mesenchymal stem-like cells to myocardial scar formation. *Purinergic Signal* 10:477–486. <https://doi.org/10.1007/s11302-014-9410-y>
17. Rossini A, Frati C, Lagrasta C, Graiani G, Scopece A, Cavalli S, Musso E, Baccarin M, Di Segni M, Fagnoni F, Germani A, Quaini E, Mayr M, Xu Q, Barbuti A, Di Francesco D, Pompilio G, Quaini F, Gaetano C, Capogrossi MC (2011) Human cardiac and bone marrow stromal cells exhibit distinctive properties related to their origin. *Cardiovasc Res* 89(3):650–660. <https://doi.org/10.1093/cvr/cvq290>
18. Vecellio M, Meraviglia V, Nanni S, Barbuti A, Scavone A, DiFrancesco D, Farsetti A, Pompilio G, Colombo GI, Capogrossi MC, Gaetano C, Rossini A (2012) In vitro epigenetic reprogramming of human cardiac mesenchymal stromal cells into functionally competent cardiovascular precursors. *PLoS One* 7:e51694. <https://doi.org/10.1371/journal.pone.0051694>

19. Terrovitis JV, Ruckdeschel Smith R, Marbàn E (2010) Assessment and optimization of cell engraftment after transplantation into the heart. *Circ Res* 106:479–494
20. Giuliani A, Mencarelli M, Frati C, Savi M, Lagrasta C, Pompilio G, Rossini A, Quani F (2018) Phase-contrast microtomography: are the tracers necessary for stem cell tracking in infarcted hearts? *Biomed. Phys Eng Express* 4 055008
21. Cancedda R, Cedola A, Giuliani A, Komlev V, Lagomarsino S, Mastrogiacomo M, Peyrin F, Rustichelli F (2007) Bulk and interface investigations of scaffolds and tissue-engineered bones by X-ray microtomography and X-ray micro-diffraction. *Biomaterials* 28:2505e24
22. Rominu M, Manescu A, Sinescu C, Negrutiu ML, Topala F, Rominu RO, Bradu A, Jackson DA, Giuliani A, Podoleanu AG (2014) Zirconia enriched dental adhesive: a solution for OCT contrast enhancement. Demonstrative study by synchrotron radiation microtomography. *Dent Mater* 30(4):417–423. <https://doi.org/10.1016/j.dental.2014.01.004>
23. Dullin C, Ufartes R, Larsson E, Martin S, Lazzarini M, Tromba G, Missbach-Guentner J, Pinkert-Leetsch D, Katschinski DM, Alves F (2017)  $\mu$ CT of ex-vivo stained mouse hearts and embryos enables a precise match between 3D virtual histology, classical histology and immunohistochemistry. *PLoS One* 12(2):e0170597. <https://doi.org/10.1371/journal.pone.0170597>
24. Giuliani A, Frati C, Rossini A, Komlev VS, Lagrasta C, Savi M, Cavalli S, Gaetano C, Quaini F, Manescu A, Rustichelli F (2011) High-resolution X-ray microtomography for three-dimensional imaging of cardiac progenitor cell homing in infarcted rat hearts. *J Tissue Eng Regen Med* 5(8):e168–e178. <https://doi.org/10.1002/term.409>
25. Giuliani A (2012) 3D visualization of transplanted stem cells in infarcted rat hearts by high-resolution X-ray microtomography. *IL NUOVO CIMENTO C* 35(5):157–167. <https://doi.org/10.1393/ncc/i2012-11318-2>
26. Kaneko Y, Shinohara G, Hoshino M, Morishita H, Morita K, Oshima Y, Takahashi M, Yagi N, Okita Y, Tsukube T (2017) Intact imaging of human heart structure using X-ray phase-contrast tomography. *Pediatr Cardiol* 38(2):390–393. <https://doi.org/10.1007/s00246-016-1527-z>
27. Arfelli F, Assante M, Bonvicini V, Bravin A, Cantatore G, Castelli E, Dalla Palma L, Di Michiel M, Longo R, Olivo A, Pani S, Pontoni D, Poropat P, Prest M, Rashevsky A, Tromba G, Vacchi A, Vallazza E, Zanconati F (1998) Low-dose phase contrast X-ray medical imaging. *Phys Med Biol* 43(10):2845–2852
28. Stokking R, Zubal IG, Viergever MA (2003) Display of fused images: methods, interpretation, and diagnostic improvements. *Semin Nucl Med* 33:219–227
29. Lang S, Zanette I, Dominietto M, Langer M, Rack A, Schulz G, Le Duc G, David C, Mohr J, Pfeiffer F, Müller B, Weitkamp T (2014) Experimental comparison of grating- and propagation-based x-ray phase tomography of soft tissue. *J Appl Phys* 116:154903. <https://doi.org/10.1063/1.4897225>
30. Izadifar M (2016) Development of nanoparticle rate-modulating and synchrotron phase contrast-based assessment techniques for cardiac tissue engineering. PhD thesis. University of Saskatchewan Saskatoon, Division of Biomedical Engineering, Saskatchewan
31. Gianella A, Guerrini U, Tilenni M, Sironi L, Milano G, Nobili E, Vaga S, Capogrossi MC, Tremoli E, Pesce M (2010) Magnetic resonance imaging of human endothelial progenitors reveals opposite effects on vascular and muscle regeneration into ischaemic tissues. *Cardiovasc Res* 85(3):503–513
32. Albertini G, Giuliani A, Komlev V, Moroncini F, Pugnalone A, Pennesi G, Belicchi M, Rubini C, Rustichelli F, Tasso R, Torrente Y (2009) Organization of extracellular matrix fibers within polyglycolic acid-poly(lactic acid) scaffolds analyzed using X-ray synchrotron-radiation phase-contrast micro computed tomography. *Tissue Eng C Methods* 15:403–411
33. Zehbe R, Haibel A, Schmidt F, Riesemeier H, Kirkpatrick CJ, Schubert H, Brochhausen C (2010) High resolution X-ray tomography – 3D imaging for tissue engineering applications. In: Eberli D (ed) *Tissue engineering*. InTech, Rijeka, pp 337–358
34. Giuliani A, Moroncini F, Mazzoni S, Belicchi ML, Villa C, Erratico S, Colombo E, Calcaterra F, Brambilla L, Torrente Y, Albertini G, Della Bella S (2014) Polyglycolic acid-poly(lactic acid) scaffold response to different progenitor cell in vitro cultures: a demonstrative and compara-

- tive X-ray synchrotron radiation phase-contrast microtomography study. *Tissue Eng Part C Methods* 20:308–316
35. İlsever M., Ünsalan C (2012) Pixel-Based Change Detection Methods. In: *Two-Dimensional Change Detection Methods*. SpringerBriefs in Computer Science. Springer, London, p 7–21
  36. Hirt MN, Hansen A, Eschenhagen T (2014) Cardiac tissue engineering. *State of the art. Circ Res* 114:354–367
  37. Rai R, Tallawi M, Barbani N, Frati C, Madeddu D, Cavalli S, Graiani G, Quaini F, Roether JA, Schubert DW, Rosellini E, Boccaccini AR (2013) Biomimetic poly(glycerol sebacate) (PGS) membranes for cardiac patch application. *Mater Sci Eng C Mater Biol Appl* 33(7):3677–3687. <https://doi.org/10.1016/j.msec.2013.04.058>
  38. Holbrook M, Clark DP, Badea CT (2018) Low-dose 4D cardiac imaging in small animals using dual source micro-CT. *Phys Med Biol* 63(2):025009
  39. Donath T, Pfeiffer F, Bunk O, Grünzweig C, Hempel E, Popescu S, Vock P, David C (2010) Toward clinical X-ray phase-contrast CT: demonstration of enhanced soft-tissue contrast in human specimen. *Investig Radiol* 45:445–452